Editors' Suggestion | Featured in Physics

# *In Situ* Imaging of the Thermal de Broglie Wavelength in an Ultracold Bose Gas

Jinggang Xiang,[1,2,3] Enid Cruz-Colón,[1,2,3] Candice C. Chua,[2,3,4] William R. Milner,[1,2,3] Julius de Hond,[1,2,3,*] Jacob F. Fricke,[1,2,3,†] and Wolfgang Ketterle[1,2,3]

[1]*Department of Physics, Massachusetts Institute of Technology, Cambridge, Massachusetts 02139, USA*
[2]*Research Laboratory of Electronics, Massachusetts Institute of Technology, Cambridge, Massachusetts 02139, USA*
[3]*MIT-Harvard Center for Ultracold Atoms, Cambridge, Massachusetts 02139, USA*
[4]*Department of Chemistry and Chemical Biology, Harvard University, Cambridge, Massachusetts 02138, USA*

(Received 13 November 2024; revised 17 January 2025; accepted 18 February 2025; published 5 May 2025)

We report the first direct *in situ* observation of density fluctuations on the scale of the thermal de Broglie wavelength in an ultracold gas of bosons. Bunching of $^{87}$Rb atoms in a quasi-two-dimensional system is observed by single-atom imaging using a quantum gas microscope. Compared to a classical ensemble, we observe a 30% enhancement of the second-order correlation function. We show the spatial and thermal dependence of these correlations. The reported method of detecting *in situ* correlations can be applied to interacting many-body systems and to the study of critical phenomena near phase transitions.

DOI: 10.1103/PhysRevLett.134.183401

*Introduction*—The original Hanbury Brown and Twiss (HBT) experiment introduced the importance of correlations in photon detection and triggered the development of quantum optics [1–4]. HBT observed a spatial correlation of the intensity fluctuations for light emitted from the distant star Sirius. These fluctuations represent an optical speckle pattern with a characteristic length scale of the optical wavelength $\lambda$ on the star's surface. As illustrated in Fig. 1, when light propagates from a distant star of radius $R$ to Earth at distance $D$, the speckle size is magnified to $\lambda D/R$ [5], which HBT determined to be around 5 m for Sirius.

Matter waves have an equivalent speckle pattern with a characteristic grain size of the thermal de Broglie wavelength $\lambda_{\mathrm{dB}} = h/\sqrt{2\pi m k_B T}$. The atomic speckle is a quantum effect, given that its scale involves Planck's constant $h$. In contrast, a classical gas has purely Poissonian fluctuations, which has no length scale since there are no correlations in the gas. Similar to light propagation, ballistic expansion of ultracold atoms magnifies the *in situ* correlation length in the far field by $D/R$ [6].

Consequently, HBT experiments have been extended beyond photons to include electrons [7–9], neutrons [10], cold atoms [11–26], and cold molecules [27]. As a result of limited detector resolution, the atomic speckle pattern has primarily been probed in the far field after time-of-flight expansion. Previous *in situ* studies have probed enhanced density fluctuations, focusing on length scales significantly larger than the de Broglie wavelength [18], temporal correlations [26], and fluctuations indirectly measured through Fourier analysis of phase-contrast images [22]. For cold fermions in a lattice, Pauli antibunching between next-neighbor sites has been observed in [28–30]. However, the counterpart of bosonic bunching is less studied. This bunching effect can be interpreted either

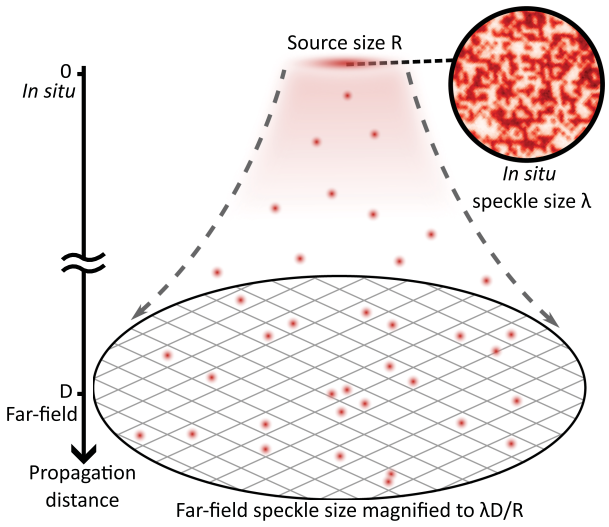


FIG. 1. *In situ* and far-field speckle patterns. An ensemble of identical bosons exhibits a spatial length scale $\lambda$ where density fluctuations are correlated. In photonic systems, the length scale of this speckle pattern is given by the optical coherence length, while for a gas of thermal atoms, it is the thermal de Broglie wavelength. In both the HBT experiment and previous cold atom experiments, a free expansion over a distance $D$ is employed to enlarge the far-field speckle size by $D/R$. In this Letter, we use a microscope with a spatial resolution smaller than the thermal de Broglie wavelength to directly image the atomic speckle *in situ*.

*Present address: Pasqal SAS, Fred. Roeskestraat 100, Amsterdam, Netherlands.
†Present address: Institute for Quantum Electronics and Quantum Center, ETH Zürich, 8093 Zürich, Switzerland.

 

as the multimode interference of matter waves or as evidence for the bosonic exchange term, which doubles the probability of simultaneously detecting two bosons at the same point.

In this Letter, we report the first direct *in situ* observation of the atomic correlation length in a bulk, thermal Bose gas. The correlations and speckle pattern are quantitatively described by the second-order correlation function $g^{(2)}$, which gives the joint probability of detecting two particles. The $g^{(2)}$ function is measured by cooling a small quasi-two-dimensional ensemble of approximately 100 rubidium atoms to below 10 nK, with a corresponding thermal de Broglie wavelength $\lambda_{\mathrm{dB}} \approx 2.3$ μm, larger than the $a_{\mathrm{lat}} = 532$ nm pinning lattice spacing used for imaging. Detection of such sparse samples is enabled by using a quantum gas microscope with single-atom resolution. Herein, we show a clear bunching signal and observe its spatial extent to be the thermal de Broglie wavelength.

*Experimental setup*—In this Letter, we extend quantum gas microscopy to a harmonically trapped bulk gas. This allows high quantum efficiency readout of atomic positions that far exceeds the signal-to-noise ratio afforded by standard *in situ* absorption imaging. Our experimental sequence begins by loading $^{87}$Rb atoms into a vertical lattice crossed with a horizontal trapping beam. The vertical lattice is created by focusing two 1064-nm beams onto the atoms that intersect at 5°, resulting in a lattice period of 12 μm. This large spacing allows the atoms to be loaded into a single layer of the vertical lattice. The combined trap is highly anisotropic, crucial for preparing a quasi-two-dimensional sample. Forced evaporative cooling is applied by gradually lowering the trap depths, resulting in final trap frequencies of $(\omega_x, \omega_y, \omega_z) = 2\pi \times (12, 15, 380)$ Hz. By fitting the density distribution, averaged over hundreds of experimental images, to a Bose-Einstein distribution in a harmonic trap, we determine the final temperature to be 6.5 nK.

When bosons are cooled below the phase transition temperature $T_c$, they form a Bose-Einstein condensate (BEC). In analogy to single-mode lasers, a BEC has $g^{(2)}(r) = 1$, identical to that of uncorrelated classical particles. This complicates the measurement of the second-order correlation function of the Bose gas due to the spatial overlap of the BEC and thermal gas. To isolate correlations in the thermal gas, we carefully control $T_c < T$ by adjusting the total atom number $N$.

During detection, we quench on a two-dimensional pinning lattice to project the bulk atomic density distribution into a square grid with 532-nm spacing. The correlation function is correspondingly discretized. Subsequently, we ramp down the vertical lattice and ramp up a light sheet for tight vertical confinement during imaging. We employ polarization gradient cooling and collect the fluorescence photons. By reconstructing fluorescence images with high fidelity, we can determine the occupancy of individual lattice sites as depicted in Fig. 2. Further experimental details can be found in Supplemental Material [31].

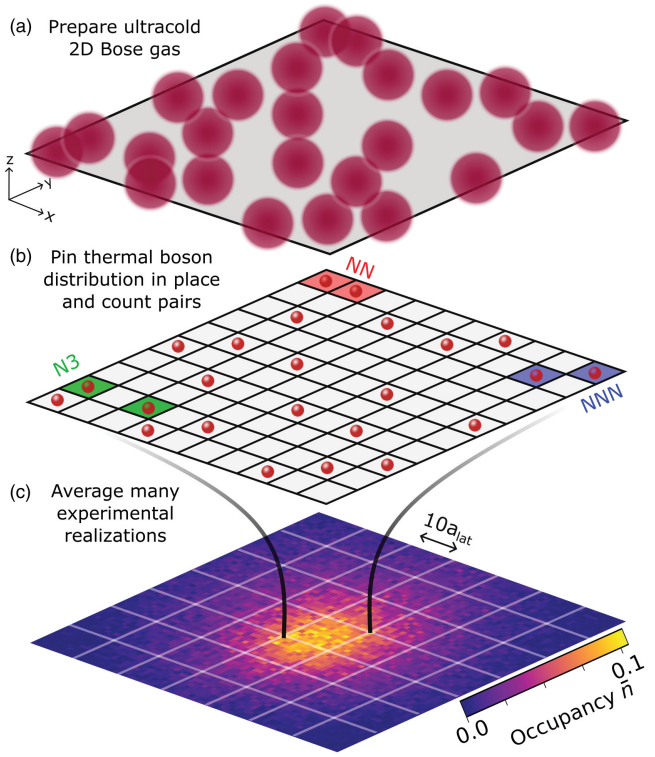


FIG. 2. Experimental overview. (a) Using a $^{87}$Rb quantum gas microscope, we probe *in situ* the density fluctuations in an ultracold, quasi-two-dimensional thermal Bose gas. (b) We project the 2D Bose distribution onto a pinning lattice and reconstruct the site-by-site lattice occupation. To determine the bosonic enhancement, we count pairs of atoms separated by distance $r$ and determine the enhancement factor $g^{(2)}(r)$ over the classical distribution corresponding to fully distinguishable particles. On the lattice grid, we show the distance between three types of pairs, corresponding to the nearest neighbor (NN, red), next-nearest neighbor (NNN, blue), and third-nearest neighbor ($N3$, green). (c) To experimentally determine $g^{(2)}(r)$ with high signal-to-noise ratio, we average over 650 experimental snapshots. The region of interest is sectioned into $10 \times 10$ boxes to address the spatial inhomogeneity of the harmonic trap. The mean occupancy $\bar{n}$ on each lattice site averaged over all snapshots is plotted. We remain dilute ($\bar{n} < 0.15$) to avoid double occupation and to ensure that we do not cross the BEC phase transition.

*Analyzing correlations*—The second-order correlation function $g^{(2)}(\mathbf{r}; \mathbf{r}')$ can be understood as the probability of jointly detecting two particles at positions $\mathbf{r}$ and $\mathbf{r}'$. For identical bosons at temperatures $T > T_c$, where the ensemble is away from the quantum critical region, the second-order correlation function has a Gaussian form that depends on the separation distance $r = |\mathbf{r} - \mathbf{r}'|$ between two particles [38],

$$g^{(2)}(r) = 1 + \exp\left(-2\pi r^2/\lambda_{\mathrm{dB}}^2\right). \tag{1}$$

When two particles occupy the same position, $g^{(2)}(0) = 2$, indicating a twofold increase in the probability of double occupation. When pairs of atoms are sufficiently far apart that there is an absence of density-density correlation between them, $g^{(2)}(r)$ decays to 1. The spatial extent of the bosonic enhancement can be characterized by the root-mean-square (rms) width of the Gaussian profile, $l = \lambda_{\mathrm{dB}}/(2\sqrt{\pi})$, which increases as the temperature of the ensemble decreases. At our measured temperature of 6.5 nK, the rms width $l$ is $1.23a_{\mathrm{lat}}$.

To statistically evaluate the bosonic enhancement, we use a simple and robust analysis method: counting pairs of atoms separated by distance $r$. The measured separation between particles is discrete due to the underlying lattice structure. The three closest types of pairs are shown in Fig. 2(b), with pair separations of 1, $\sqrt{2}$, and 2 $a_{\mathrm{lat}}$, respectively. When the distance between atoms on two distinct lattice sites is within the thermal de Broglie wavelength, there will be an enhancement in the number of detected pairs compared to the classical expectation value.

For particles on a lattice site with indices $(i, j)$, the NN pair corresponds to sites $(i \pm 1, j)$ and $(i, j \pm 1)$. In a homogeneous region of interest of $m \times m$ sites, assuming the probability of detecting one particle per site to be $p$, the expectation value for the number of classical (distinguishable) NN pairs is $2m(m-1)p^2$. The $-1$ accounts for the fact that the region of interest is finite and the correction varies as the pair separation increases. For indistinguishable particles, the expectation value for the number of NN pairs is $g^{(2)}(r = a_{\mathrm{lat}}) \times 2m(m-1)p^2$. In the absence of technical corrections, the ratio of measured pairs to classically expected pairs gives the second-order correlation function $g^{(2)}(r)$.

Ideally, we would probe the $g^{(2)}$ function at $r = 0$, where the correlation signal is strongest. However, due to light-assisted collisions characteristic of quantum gas microscopes, double occupation on a single lattice site is parity projected to an empty site. Detecting pairs at $r = 0$ requires doublon detection schemes [30,39–41], which we do not implement in this Letter. The smallest separation we probe is $r = a_{\mathrm{lat}}$ and the largest is $r \approx 5$ μm.

Since the quasi-two-dimensional cloud is prepared in a harmonic trap, the probability of detecting one particle per site has spatial dependence. We divide the total field of $70 \times 70$ sites into 49 smaller boxes of $10 \times 10$ sites, as illustrated in Fig. 2(c). This is directly analogous to applying the local-density approximation, where locally homogeneous regions are sampled. Within a $10 \times 10$ box, there is a residual spatial inhomogeneity that grows quadratically to ≈10% for pairs separated by 5 μm. We determine the magnitude of this correction from a numerical simulation of our experimental density [31] and experimentally confirm this correction with a high-temperature measurement where correlations are minimal.

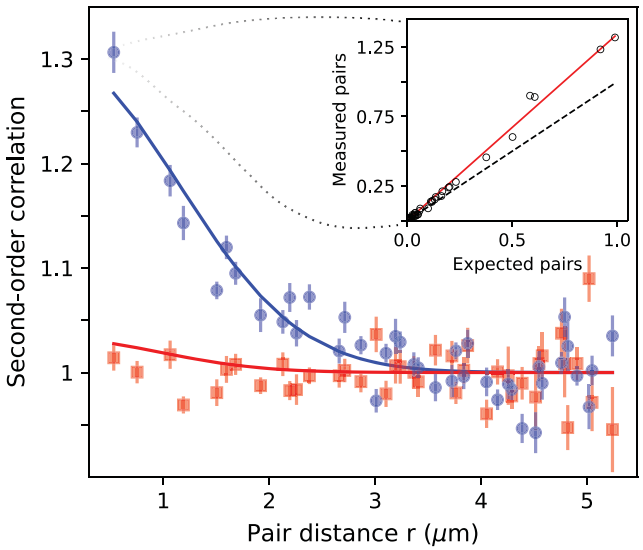


FIG. 3. Spatial and thermal dependence of the second-order correlation function. $g^{(2)}(r)$ correlations determined from *in situ* microscope images are plotted for ensembles at temperatures $T = 6.5$ nK (blue circle) and 54 nK (red square), respectively. The solid lines are fits using Eq. (2), including corrections for higher motional $n_z$ states and pinning lattice blurring. The thermal de Broglie wavelength is a fixed parameter. Both datasets are normalized by the mean of measurements at distance $r > 3$ μm, where no correlations are expected. Inset: for NN pairs, the number of measured pairs in $10 \times 10$ regions [see Fig. 2(c)] are plotted against the classical expectations. The red solid line is a linear fit to the data, while the black dashed line is the classical expectation. The fitted slope directly gives $g^{(2)}(r = a_{\mathrm{lat}})$, and the standard deviation of the fitted slope is used as the error bar in the main plot.

Temporal atom number fluctuations between experimental snapshots are also a noise source that will enhance the number of observed pairs. This effect does not depend on the pair separation distance $r$ and only adds an overall scaling factor to the absolute value of $g^{(2)}(r)$. A detailed explanation can be found in Supplemental Material [31]. While this effect can be mitigated by postselecting data based on the total atom number [27], instead, we choose to include all data but normalize $g^{(2)}(r)$ by the pairs separated at a distance larger than 3 μm, where density fluctuations are uncorrelated.

*Results*—We implement our pair analysis technique to determine the spatial second-order correlation for our thermal Bose gas, presented in Fig. 3. At each discrete pair separation, we evaluate the pair enhancement. For a sample prepared at 6.5 nK, we observe a 31(2)% increase in the second-order correlation function for nearest-neighbor pairs separated by $a_{\mathrm{lat}}$, as plotted in the Fig. 3 inset. The spatial dependence matches the theoretical prediction with the thermal de Broglie wavelength $\lambda_{\mathrm{dB}}$ being 2.3 μm. In contrast, when we prepare a cloud at a higher temperature of

54 nK, the observed second-order correlations are strongly diminished.

When extrapolated to $r = 0$, the observed correlation function $g^{(2)}_{\mathrm{obs}}(r)$ for the cold sample approaches a value of 1.3, rather than the expected value of 2. This can be attributed to the finite spatial resolution of the pinning lattice and the fact that the system is not truly two dimensional. Our systematic understanding of this reduction can be described by the following function:

$$g^{(2)}_{\mathrm{obs}}(r) = 1 + \eta \frac{l^2}{\tilde{l}^2} \exp\left[-\frac{r^2}{2\tilde{l}^2}\right]. \tag{2}$$

In this expression, $\eta$ accounts for effects that display a global reduction of $g^{(2)}_{\mathrm{obs}}(r) - 1$ (independent of $r$). The finite spatial resolution $\sigma$ of the underlying pinning lattice [6] broadens the correlation length $l$ to $\tilde{l} = \sqrt{l^2 + (\sqrt{2}\sigma)^2}$.

When using a pinning lattice to probe free-space atoms, the spatial resolution is not limited by the optical resolution, as long as high-fidelity image reconstruction is achieved under the quantum gas microscope. However, due to the discretized nature of the pinning lattice, the atom's position cannot be resolved beyond the lattice spacing. Consequently, the observed density distribution is the convolution of the true continuous density distribution with the lattice-imposed spatial resolution [6,13]. This effect broadens the profile of $g^{(2)}_{\mathrm{obs}}(r)$ and lowers its value at $r = 0$.

When atoms are projected onto a lattice with period $a_{\mathrm{lat}}$, the point spread function of a simple classical model is a boxcar function with a full width at half maximum (FWHM) of $a_{\mathrm{lat}}$, which corresponds to an rms width of $\sigma_{\mathrm{classical}} = a_{\mathrm{lat}}/\sqrt{12}$. For the distance between two atoms, the instrumental function is the convolution of this box with itself, producing a triangular function of FWHM $a_{\mathrm{lat}}$ (rms width $a_{\mathrm{lat}}/\sqrt{6}$). We model our resolution as a Gaussian with an effective rms width $\sigma$. The rms length of the measured second-order correlation function is broadened to $\tilde{l} = \sqrt{l^2 + (\sqrt{2}\sigma)^2}$, where the $\sqrt{2}$ factor reflects the spatial resolution for detecting two-particle correlations. We fit our data using Eq. (2), where we fix $\eta$ from independent measurements and use only $\sigma$ as an adjustable parameter. We obtain $\sigma = 1.25 a_{\mathrm{lat}}$. The additional broadening compared to the classical limit is likely caused by the dynamics during the fast lattice ramp, as this can cause atoms to be excited to higher bands and have significant tunneling rates [42,43]. It is an interesting question for future research to determine the ultimate quantum point spread function for a quantum gas microscope.

Even with perfect spatial resolution, the amplitude of $g^{(2)}_{\mathrm{obs}}(r)$ can be reduced by line-of-sight integration, as we are probing a quasi-two-dimensional sample. This effect does not broaden the profile of $g^{(2)}_{\mathrm{obs}}(r)$ and is represented by the $\eta$ factor in Eq. (2). In a purely two-dimensional gas, where only the ground state of the vertical trapping potential is populated, this effect would be eliminated. Under our experimental conditions ($\omega_z = 2\pi \times 380$ Hz, $T = 6.5$ nK), approximately 95% of atoms are in the ground state of the vertical trap, resulting in a contrast reduction by a factor of $\eta = 0.91$. This reduction occurs because atoms in different $n_z$ states are "distinguishable" and therefore uncorrelated.

Another fundamental reduction of the contrast is due to the effect of finite particle numbers [31,44]. As the enhanced correlations are due to exchange terms, they are reduced by $(N-1)/N$, as there is no exchange of a boson with itself. More importantly, near the phase transition, the lowest states are already populated with multiple atoms, and this reduces the exchange terms further. For a two-dimensional box potential with $N \approx 100$, we estimate the contrast reduction to be $\approx 7\%$ [31]. This effect does not significantly change our conclusions and, therefore, is not included in the fit. The effect becomes more pronounced with fewer atoms or closer proximity to the phase transition.

We also observe the temperature dependence of the second-order correlation function. By raising the vertical lattice nonadiabatically to heat the cloud, we measure a higher temperature of 54 nK, corresponding to a thermal de Broglie wavelength $\lambda_{\mathrm{dB}}$ of 0.81 μm and an rms width $l$ of $0.43 a_{\mathrm{lat}}$. As shown in Fig. 3, the enhancement of the second-order correlation is substantially reduced and no longer statistically significant. The fact that the function is almost flat at $g^{(2)}_{\mathrm{obs}}(r) \approx 1$ confirms our normalization procedure. The high-temperature data are consistent with the red curve, which is obtained without any free fitting parameters.

*Outlook*—We have directly probed the bosonic correlation length *in situ* for the first time through the measurement of the second-order correlation function. We report a clear enhancement compared to the classically expected value and discuss key sources of contrast reduction. Future work can be extended in many different directions. With a homogeneous potential, one could observe modifications of the correlation function near the BEC phase transition, where the correlation length diverges and a power law decay is expected [45]. In the future, implementing doublon detection [30,39–41] could allow the study of correlations at $r = 0$, where we expect to see the strongest correlation signal, and possibly also allow the probing of interaction effects that are negligible on the length scales in this study. Such interaction effects become dominant in a Tonks gas [46], which could also be studied *in situ* with our technique.

*Note added*—Recently, we became aware of the following Letters on *in situ* studies of correlations in ultracold Fermi and Bose gases [47,48].

*Acknowledgments*—We acknowledge Woo Chang Chung for early contributions to the design of the quantum gas microscope, Hanzhen Lin for experimental assistance, and Yoo Kyung Lee and Yu-Kun Lu for critical reading of the manuscript. We acknowledge support from the NSF through Grant No. PHY-2208004, the Center for Ultracold Atoms (an NSF Physics Frontiers Center) through Grant No. PHY-2317134, and the Army Research Office (Award No. W911NF-24-1-0218, Grant No. W911NF-22-1-0024, DURIP).

[1] R. Hanbury Brown and R. Q. Twiss, Nature (London) **177**, 27 (1956).
[2] R. Hanbury Brown and R. Q. Twiss, Nature (London) **178**, 1046 (1956).
[3] R. J. Glauber, Phys. Rev. **131**, 2766 (1963).
[4] R. J. Glauber, Phys. Rev. **130**, 2529 (1963).
[5] A. Aspect, arXiv:2005.08239.
[6] J. V. Gomes, A. Perrin, M. Schellekens, D. Boiron, C. I. Westbrook, and M. Belsley, Phys. Rev. A **74**, 053607 (2006).
[7] W. D. Oliver, J. Kim, R. C. Liu, and Y. Yamamoto, Science **284**, 299 (1999).
[8] M. Henny, S. Oberholzer, C. Strunk, T. Heinzel, K. Ensslin, M. Holland, and C. Schönenberger, Science **284**, 296 (1999).
[9] H. Kiesel, A. Renz, and F. Hasselbach, Nature (London) **418**, 392 (2002).
[10] M. Iannuzzi, A. Orecchini, F. Sacchetti, P. Facchi, and S. Pascazio, Phys. Rev. Lett. **96**, 080402 (2006).
[11] M. Yasuda and F. Shimizu, Phys. Rev. Lett. **77**, 3090 (1996).
[12] R. G. Dall, S. S. Hodgman, A. G. Manning, M. T. Johnsson, K. G. H. Baldwin, and A. G. Truscott, Nat. Commun. **2**, 291 (2011).
[13] M. Schellekens, R. Hoppeler, A. Perrin, J. V. Gomes, D. Boiron, A. Aspect, and C. I. Westbrook, Science **310**, 648 (2005).
[14] T. Jeltes, J. M. McNamara, W. Hogervorst, W. Vassen, V. Krachmalnicoff, M. Schellekens, A. Perrin, H. Chang, D. Boiron, A. Aspect, and C. I. Westbrook, Nature (London) **445**, 402 (2007).
[15] A. G. Manning, S. S. Hodgman, R. G. Dall, M. T. Johnsoon, and A. G. Truscott, Opt. Express **18**, 18712 (2010).
[16] A. G. Manning, W. RuGway, S. S. Hodgman, R. G. Dall, K. G. H. Baldwin, and A. G. Truscott, New J. Phys. **15**, 013042 (2013).
[17] K. F. Thomas, S. Li, A. H. Abbas, A. G. Truscott, and S. S. Hodgman, Phys. Rev. Res. **6**, L022003 (2024).
[18] J. Esteve, J.-B. Trebbia, T. Schumm, A. Aspect, C. I. Westbrook, and I. Bouchoule, Phys. Rev. Lett. **96**, 130403 (2006).
[19] A. Perrin, R. Bücker, S. Manz, T. Betz, C. Koller, T. Plisson, T. Schumm, and J. Schmiedmayer, Nat. Phys. **8**, 195 (2012).
[20] S. Sunami, V. P. Singh, E. Rydow, A. Beregi, E. Chang, L. Mathey, and C. J. Foot, arXiv:2406.03491.
[21] S. Fölling, F. Gerbier, A. Widera, O. Mandel, T. Gericke, and I. Bloch, Nature (London) **434**, 481 (2005).
[22] A. Blumkin, S. Rinott, R. Schley, A. Berkovitz, I. Shammass, and J. Steinhauer, Phys. Rev. Lett. **110**, 265301 (2013).
[23] T. Rom, T. Best, D. Van Oosten, U. Schneider, S. Fölling, B. Paredes, and I. Bloch, Nature (London) **444**, 733 (2006).
[24] C. Sanner, E. J. Su, A. Keshet, R. Gommers, Y.-i. Shin, W. Huang, and W. Ketterle, Phys. Rev. Lett. **105**, 040402 (2010).
[25] T. Müller, B. Zimmermann, J. Meineke, J.-P. Brantut, T. Esslinger, and H. Moritz, Phys. Rev. Lett. **105**, 040401 (2010).
[26] V. Guarrera, P. Würtz, A. Ewerbeck, A. Vogler, G. Barontini, and H. Ott, Phys. Rev. Lett. **107**, 160403 (2011).
[27] J. S. Rosenberg, L. Christakis, E. Guardado-Sanchez, Z. Z. Yan, and W. S. Bakr, Nat. Phys. **18**, 1062 (2022).
[28] L. W. Cheuk, M. A. Nichols, M. Okan, T. Gersdorf, V. V. Ramasesh, W. S. Bakr, T. Lompe, and M. W. Zwierlein, Phys. Rev. Lett. **114**, 193001 (2015).
[29] A. Omran, M. Boll, T. A. Hilker, K. Kleinlein, G. Salomon, I. Bloch, and C. Gross, Phys. Rev. Lett. **115**, 263001 (2015).
[30] T. Hartke, B. Oreg, N. Jia, and M. Zwierlein, Phys. Rev. Lett. **125**, 113601 (2020).
[31] See Supplemental Material at http://link.aps.org/supplemental/10.1103/PhysRevLett.134.183401 for details on the experimental setup and finite size effects, which includes Refs. [32–37].
[32] E. W. Streed, A. P. Chikkatur, T. L. Gustavson, M. Boyd, Y. Torii, D. Schneble, G. K. Campbell, D. E. Pritchard, and W. Ketterle, Rev. Sci. Instrum. **77** (2006).
[33] W. Ketterle and N. J. van Druten, Phys. Rev. A **54**, 656 (1996).
[34] Z. Hadzibabic and J. Dalibard, Riv. Nuovo Cimento Soc. Ital. Fis. **34**, 389 (2011).
[35] J. T. M. Walraven, Atomic Hydrogen in Magnetostatic Traps, pg. 16, Eq. 2.32 (1996), https://staff.science.uva.nl/j.t.m.walraven/walraven/Publications_files/StirlingPaper.pdf.
[36] M. Wilkens and C. Weiss, J. Mod. Opt. **44**, 1801 (1997).
[37] V. V. Kocharovsky, V. V. Kocharovsky, M. Holthaus, C. R. Ooi, A. Svidzinsky, W. Ketterle, and M. O. Scully, Adv. At. Mol. Opt. Phys. **53**, 291 (2006).
[38] M. Naraschewski and R. J. Glauber, Phys. Rev. A **59**, 4595 (1999).
[39] C. Gross and W. S. Bakr, Nat. Phys. **17**, 1316 (2021).
[40] P. M. Preiss, R. Ma, M. E. Tai, J. Simon, and M. Greiner, Phys. Rev. A **91**, 041602 (2015).
[41] J. Koepsell, S. Hirthe, D. Bourgund, P. Sompet, J. Vijayan, G. Salomon, C. Gross, and I. Bloch, Phys. Rev. Lett. **125**, 010403 (2020).
[42] J. Verstraten, K. Dai, M. Dixmerias, B. Peaudecerf, T. de Jongh, and T. Yefsah, Phys. Rev. Lett. **134**, 083403 (2025).
[43] M. Pyzh, S. Krönke, C. Weitenberg, and P. Schmelcher, New J. Phys. **21**, 053013 (2019).

[44] T. M. Wright, A. Perrin, A. Bray, J. Schmiedmayer, and K. V. Kheruntsyan, Phys. Rev. A **86**, 023618 (2012).
[45] Y.-K. Lu, Y. Margalit, and W. Ketterle, Nat. Phys. **19**, 210 (2023).
[46] Y. Hao, Y. Zhang, Y. Liu, and L. Wang, Eur. Phys. J. D **76**, 237 (2022).
[47] T. de Jongh, J. Verstraten, M. Dixmerias, C. Daix, B. Peaudecerf, and T. Yefsah, companion Letter, Phys. Rev. Lett. **134**, 183403 (2025).
[48] R. Yao, S. Chi, M. Wang, R. J. Fletcher, and M. Zwierlein, companion Letter, Phys. Rev. Lett. **134**, 183402 (2025).